Symplectic Time-Stepping for Particle Methods

Matthew Dixon* and **Sebastian Reich****

Department of Mathematics, Imperial College London, London SW7 2AZ, England

This paper surveys some of the fundamental properties of symplectic integration schemes for classical mechanics and particle methods in particular. The widely used Störmer-Verlet method is discussed in detail and implications of conservation of symplecticity on long term simulations are outlined. The second part of the paper describes the application of a Lagrangian particle method and the Störmer-Verlet time integrator to numerical weather prediction (NWP). A simple vertical slice model and non-hydrostatic flow over orography are discussed in detail.

1 Introduction

This survey is intended to provide an introduction to the concept of symplectic time integration as applicable to conservative systems of interacting particles. Such particle systems arise in the context of molecular dynamics [13, 1], astrophysics [26, 16], plasmaphysics [22], and fluid dynamics [33, 14]. Conservation of important physical quantities such as energy and momentum are crucial for long time simulations; these conservation laws are represented by a rich symmetry structure in the symplectic time-stepping algorithms which is both mathematically elegant and physically intuitive [34, 20, 25]. We will demonstrate this for the Störmer-Verlet method [34, 20, 25], which is the most popular symplectic integration method, in §3.

Throughout the survey, we will consider systems of N particles which interact through Newton's 2nd law:

$$\dot{\mathbf{r}}_i = \mathbf{p}_i/m_i, \tag{1}$$

$$\dot{\mathbf{p}}_i = \mathbf{F}_i, \qquad i = 1, \ldots, N \tag{2}$$

where m_i is the mass of particle i with position vector $\mathbf{r}_i = (x_i, y_i, z_i)^T \in \mathbb{R}^3$ and momentum $\mathbf{p}_i = m_i \dot{\mathbf{r}}_i \in \mathbb{R}^3$. It is also assumed that the force $\mathbf{F}_i$ acting on the i^{th} particle is conservative; *i.e.*, can be derived from a potential energy function.

We begin the survey by introducing the concepts of Hamiltonian dynamics and symplecticity. We continue with the discussion of the symplectic Störmer-Verlet method and its numerical properties in terms of backward error analysis. The rest of the survey is then devoted to *numerical weather prediction* (NWP) as an emerging application area for *particle methods* and *symplectic time integration*.

* e-mail: matthew.dixon@imperial.ac.uk
** corresponding author, e-mail: s.reich@imperial.ac.uk

2 Hamiltonian Dynamics and the Symplectic Form

For a particle system with conservative forces

$$\mathbf{F}_i = -\nabla_{\mathbf{r}_i} V(\mathbf{r}_1, \ldots, \mathbf{r}_N)$$

(where $V(\mathbf{r}_1, \ldots, \mathbf{r}_N)$ is some potential energy function) the equations of motion (1)-(2) conserve total energy

$$\mathcal{H} = \frac{1}{2} \sum_{i=1}^{N} \|\mathbf{p}_i\|^2 / m_i + V(\mathbf{r}_1, \ldots, \mathbf{r}_N). \tag{3}$$

Here $\nabla_{\mathbf{r}_i} V(\mathbf{r}) \in \mathbb{R}^3$ represents the column vector of partial derivatives given by

$$\nabla_{\mathbf{r}_i} V(\mathbf{r}) = (\partial_{x_i} V(\mathbf{r}), \partial_{y_i} V(\mathbf{r}), \partial_{z_i} V(\mathbf{r}))^T, \qquad \mathbf{r} = (\mathbf{r}_1^T, \ldots, \mathbf{r}_N^T)^T.$$

The conservative nature of the forces has important implications for the design of practical numerical methods for particle methods. It is easily verified that equations (1)-(2) are equivalent to the more abstract formulation

$$\dot{\mathbf{r}}_i = +\nabla_{\mathbf{p}_i} \mathcal{H}, \qquad \dot{\mathbf{p}}_i = -\nabla_{\mathbf{r}_i} \mathcal{H}, \tag{4}$$

$i = 1, \ldots, N$, where the *Hamiltonian function* $\mathcal{H}$ is given by (3). Hence particle methods fall into the category of *Hamiltonian mechanics* [3]. This observation has important implications for the numerical treatment relating to the *symplectic structure* of Hamiltonian mechanics [3, 25]. To see this symplectic structure, take a solution $(\mathbf{r}_i(t), \mathbf{p}_i(t))$, $i = 1, \ldots, N$, of the equations (1)-(2) and linearize (1)-(2) along that solution to obtain the following time-dependent linear equations

$$\dot{\mathbf{R}}_i = \mathbf{P}_i / m_i, \tag{5}$$

$$\dot{\mathbf{P}}_i = -\sum_{j=1}^{N} \mathbf{A}_{ij}(t)\, \mathbf{R}_j \tag{6}$$

in the variables $\mathbf{R}_i \in \mathbb{R}^3$, $\mathbf{P}_i \in \mathbb{R}^3$, where

$$\mathbf{A}_{ij}(t) = D_{\mathbf{r}_i \mathbf{r}_j} V(\mathbf{r}_1(t), \ldots, \mathbf{r}_n(t))$$

is a symmetric, time-dependent 3×3 matrix of second order partial derivatives of V with respect to $\mathbf{r}_i$ and $\mathbf{r}_j$. Let $(\mathbf{R}_i^{(1)}(t), \mathbf{P}_i^{(1)}(t))$ and $(\mathbf{R}_i^{(2)}(t), \mathbf{P}_i^{(2)}(t))$ denote any two solutions of (5)-(6). Then it is easy to check that

$$\frac{d}{dt} \left[\sum_{i=1}^{N} \mathbf{R}_i^{(1)}(t) \cdot \mathbf{P}_i^{(2)}(t) - \mathbf{R}_i^{(2)}(t) \cdot \mathbf{P}_i^{(1)}(t) \right] = 0.$$

The expression in the bracket is linear in each of the arguments and defines a two-form Ω called the *symplectic form*. Hence the more abstract property of *conservation of symplecticity* $\dot{\Omega} = 0$ is derived. (See the Appendix for a precise definition and more

details.) A consequence of conservation of symplecticity is conservation of volume in phase space [3].

Additional conservation properties may apply. For example, consider a particle system with a pairwise force $\mathbf{F}_{ij}$ acting on particle i due to particle j and

$$\mathbf{F}_i = \sum_{j=1}^{N} \mathbf{F}_{ij}.$$

A wide range of the potential energy functions commonly used in particle methods lead to interactions that furthermore satisfy Newton's third law:

$$\mathbf{F}_{ij} = -\mathbf{F}_{ji}$$

and the force $\mathbf{F}_{ij}$ acts into the direction of $\mathbf{r}_{ij} = \mathbf{r}_i - \mathbf{r}_j$. The immediate consequence is that such systems conserve total linear and angular momentum:

$$\mathbf{P} = \sum_{i=1}^{N} \mathbf{p}_i, \qquad \mathbf{L} = \sum_{i=1}^{N} \mathbf{r}_i \times \mathbf{p}_i.$$

3 The Symplectic Störmer-Verlet Algorithm

Let us rewrite equations (4) in the more compact form

$$\dot{\mathbf{r}} = +\nabla_{\mathbf{p}} \mathcal{H}, \qquad \dot{\mathbf{p}} = -\nabla_{\mathbf{r}} \mathcal{H}, \tag{7}$$

with $\mathbf{p} = (\mathbf{p}_1^T, \ldots, \mathbf{p}_N^T)^T$, $\mathbf{r} = (\mathbf{r}_1^T, \ldots, \mathbf{r}_N^T)^T$ as defined before, the Hamiltonian (3) equivalent to

$$\mathcal{H} = \frac{1}{2}\mathbf{p}^T \mathbf{M}^{-1} \mathbf{p} + V(\mathbf{r}),$$

and $\mathbf{M}$ a diagonal mass matrix.

The most widely used numerical method for equations of type (7) is the *Störmer-Verlet* method, which is written here in the momentum formulation:

$$\mathbf{p}^{n+1/2} = \mathbf{p}^n - \frac{\Delta t}{2} \nabla_{\mathbf{r}} V(\mathbf{r}^n), \tag{8}$$

$$\mathbf{r}^{n+1} = \mathbf{r}^n + \Delta t \mathbf{M}^{-1} \mathbf{p}^{n+1/2}, \tag{9}$$

$$\mathbf{p}^{n+1} = \mathbf{p}^{n+1/2} - \frac{\Delta t}{2} \nabla_{\mathbf{r}} V(\mathbf{r}^{n+1}), \tag{10}$$

where Δt is the step size. There is evidence that the method was already known to Newton and used in his *Principia* from 1687 to prove Kepler's second law (see [21]).

There exist a number of essentially equivalent formulations of the Störmer-Verlet method. See, for example, SCHLICK [35]. Introduce the abbreviation *kick* for the momentum updates (8) and (10), and the abbreviation *drift* for the position update (9). Hence the momentum Störmer-Verlet method may be characterized as *kick-drift-kick*.

Why is the Störmer-Verlet method so successful for conservative particle systems? Several reasons can be given. The method is easy to implement, it exactly conserves total linear and angular momentum, it is time-reversible, and the total energy (3) is very well conserved over long simulation times even for large and complex systems.

In fact, taking a slightly different perspective, these conservation properties become less of a surprise. Recall that the equations of motion can be derived from the Hamiltonian function (3). Write the Hamiltonian function $\mathcal{H}$ as the sum of three parts

$$\mathcal{H}_1 = \frac{1}{2}V(\mathbf{r}), \qquad \mathcal{H}_2 = \frac{1}{2}\mathbf{p}^T\mathbf{M}^{-1}\mathbf{p}, \qquad \mathcal{H}_3 = \frac{1}{2}V(\mathbf{r}).$$

Taking each of these terms separately to be the Hamiltonian function of a Hamiltonian system gives rise to equations of motion with trivial dynamics. For example, take the Hamiltonian $\mathcal{H}_1$. The associated equations are

$$\dot{\mathbf{p}} = -\frac{1}{2}\nabla_{\mathbf{r}}V(\mathbf{r}), \qquad \dot{\mathbf{r}} = \mathbf{0}.$$

These equations can be solved analytically, producing the momentum update (*kick*):

$$\mathbf{p}(t) = \mathbf{p}(0) - \frac{t}{2}\nabla_{\mathbf{r}}V(\mathbf{r}), \qquad \mathbf{r}(t) = \mathbf{r}(0).$$

Denote the associated map from time $t = 0$ to $t = \tau$ by $\Psi_{\tau,\mathcal{H}_1} : (\mathbf{r}(0), \mathbf{p}(0)) \to (\mathbf{r}(\tau), \mathbf{p}(\tau))$. Similarly $\Psi_{\tau,\mathcal{H}_3} = \Psi_{\tau,\mathcal{H}_1}$ and $\Psi_{\tau,\mathcal{H}_2}$ is easily calculated to be the position update (*drift*):

$$\mathbf{p}(\tau) = \mathbf{p}(0), \qquad \mathbf{r}(\tau) = \mathbf{r}(0) + \tau\mathbf{M}^{-1}\mathbf{p}(0).$$

Now, if one applies the map $\Psi_{\tau,\mathcal{H}_1}$ with $\tau = \Delta t$ to the numerical approximation $(\mathbf{r}^n, \mathbf{p}^n)$ and calls the result $(\mathbf{r}^n, \mathbf{p}^{n+1/2})$, and then applies $\Psi_{\Delta t,\mathcal{H}_2}$ to that approximation followed by an application of $\Psi_{\Delta t,\mathcal{H}_3}$, then the result $(\mathbf{r}^{n+1}, \mathbf{p}^{n+1})$ is exactly equivalent to the outcome from the Störmer-Verlet method (8)-(10). Hence the Störmer-Verlet method may be written as a map $\Phi_{\Delta t} : (\mathbf{r}^n, \mathbf{p}^n) \to (\mathbf{r}^{n+1}, \mathbf{p}^{n+1})$ which itself is a concatenation of three maps:

$$\Phi_{\Delta t} = \Psi_{\Delta t,\mathcal{H}_3} \circ \Psi_{\Delta t,\mathcal{H}_2} \circ \Psi_{\Delta t,\mathcal{H}_1}.$$

In other words, each of the three maps corresponds to exactly one step in the *kick-drift-kick* sequence of the Störmer-Verlet method (8)-(10). A number of very useful conclusions can be drawn from this abstract result.

(i) Each map $\Psi_{\Delta t,\mathcal{H}_i}$ conserves total linear and angular momentum. Hence the composition of these maps (*i.e.* the Störmer-Verlet method) conserves total linear and angular momentum.

(ii) Each map $\Psi_{\Delta t,\mathcal{H}_i}$ is the exact solution to a Hamiltonian differential equation and thus conserves the symplectic two-form Ω introduced in §2 (see also the Appendix). Hence the Störmer-Verlet method preserves the symplectic two-form Ω from time step to time step, *i.e.* $\Omega^{n+1} = \Omega^n$. A numerical integrator with this property is called a *symplectic method* [34, 20, 25].

(iii) Time-reversibility of the Störmer-Verlet method follows from the obvious symmetry property

$$\Psi_{\Delta t,\mathcal{H}_3} \circ \Psi_{\Delta t,\mathcal{H}_2} \circ \Psi_{\Delta t,\mathcal{H}_1} = \Psi_{\Delta t,\mathcal{H}_1} \circ \Psi_{\Delta t,\mathcal{H}_2} \circ \Psi_{\Delta t,\mathcal{H}_3}$$

in the composition of the three flow maps. This symmetry also implies that the Störmer-Verlet method is second order.

We next describe a truly remarkable observation for the Störmer-Verlet method which relies on its conservation of the symplectic two-form Ω. Namely, one can find a time-dependent Hamiltonian function $\tilde{\mathcal{H}}(\mathbf{r},\mathbf{p},2\pi\, t/\Delta t)$ which is 2π-periodic in its third argument such that the solution of

$$\begin{aligned} \dot{\mathbf{r}} &= +\nabla_{\mathbf{p}}\tilde{\mathcal{H}}(\mathbf{r},\mathbf{p},2\pi\, t/\Delta t), \\ \dot{\mathbf{p}} &= -\nabla_{\mathbf{r}}\tilde{\mathcal{H}}(\mathbf{r},\mathbf{p},2\pi\, t/\Delta t) \end{aligned}$$

with initial conditions $\mathbf{r}(0)=\mathbf{r}^n$ and $\mathbf{p}(0)=\mathbf{p}^n$ is exactly equivalent to $(\mathbf{r}^{n+1},\mathbf{p}^{n+1})$ at $t=\Delta t$. (See the paper by Kuksin & Pöschel [24] and Moan [28] for the mathematical details.) Using a more abstract notation, we can state

$$\Phi_{\Delta t} = \Psi_{\Delta t,\tilde{\mathcal{H}}}.$$

This result tells us that the solution behaviour of the Störmer-Verlet method is completely characterized by a *time-dependent* Hamiltonian problem with Hamiltonian function $\tilde{\mathcal{H}}$.

This statement is not entirely satisfactory as it is well known that energy is *not* conserved for time-dependent Hamiltonian problems. However, as first pointed out by Neishtadt [30], the time-dependence in $\tilde{\mathcal{H}}$ averages itself out up to negligible terms of size $\mathcal{O}(e^{-c/\Delta t})$ for sufficiently small step-sizes Δt (here $c>0$ is a constant which depends on the particular problem). Hence we can claim that the Störmer-Verlet method is the nearly exact solution of a Hamiltonian problem with *time-independent* Hamiltonian $\hat{\mathcal{H}}_{\Delta t}(\mathbf{r},\mathbf{p})$. This time-independent Hamiltonian possesses an asymptotic expansion in the step-size Δt of the form

$$\hat{\mathcal{H}}_{\Delta t} = \mathcal{H} + \Delta t^2\delta\mathcal{H}_2 + \Delta t^4\delta\mathcal{H}_4 + \Delta t^6\mathcal{H}_6 + \ldots,$$

with

$$\mathcal{H}_2 = \frac{1}{12}\mathbf{p}^T\mathbf{M}^{-1}[D_{\mathbf{rr}}V(\mathbf{r})]\mathbf{M}^{-1}\mathbf{p} + \frac{1}{24}[\nabla_{\mathbf{r}}V(\mathbf{r})]^T\mathbf{M}^{-1}\nabla_{\mathbf{r}}V(\mathbf{r}),$$

where $D_{\mathbf{rr}}V(\mathbf{r})$ denotes the $3N\times 3N$ Hessian matrix of the potential energy V. Expressions for the higher order correction terms $\delta\mathcal{H}_i$, $i=4,6,\ldots$, can be found using the Baker-Campbell-Hausdorff (BCH) formula (see [34], [20], or [25]).

A practical algorithm for assessing energy conservation with respect to a modified Hamiltonian has been proposed by Skeel & Hardy [36]. See also [29] for an easier construction particularly suited to the Störmer-Verlet method.

The fact that the modified energy $\tilde{\mathcal{H}}_{\Delta t}$ is essentially preserved exactly under the Störmer-Verlet method and the fact that

$$|\mathcal{H} - \hat{\mathcal{H}}_{\Delta t}| = \mathcal{O}(\Delta t^2)$$

explains the observed approximate conservation of energy under the Störmer-Verlet method. See Benettin & Giorgilli [4], Hairer & Lubich [19] and Reich [32] for rigorous results.

In many practical applications, such as molecular dynamics and numerical weather prediction, the initial state $(\mathbf{r}_0, \mathbf{p}_0)$ of a system is not known exactly. In such circumstances it makes more sense to consider an initial probability distribution function (PDF) $\rho_0(\mathbf{r}, \mathbf{p})$, which is centered about the expected initial state $(\mathbf{r}_0, \mathbf{p}_0)$. Hence one is led to actually consider the time evolution of this initial PDF under the given Hamiltonian equations of motion. Using flow map notation this can be written as

$$\rho(t) = \rho_0 \circ \Psi_{t,\mathcal{H}}$$

for the analytic problem and

$$\tilde{\rho}(t_n) = \rho_0 \circ \Psi_{t_n,\tilde{\mathcal{H}}}$$

for the Störmer-Verlet method. The 'observed' value of an observable A, such as temperature or pressure, is now defined at any time t as the spatial average of A with respect to $\rho(t)$:

$$\langle A \rangle(t) = \int A\, \rho(t)\, d\mathbf{r} d\mathbf{p}.$$

This average gets replaced by

$$\langle \tilde{A} \rangle(t_n) = \int A\, \tilde{\rho}(t_n)\, d\mathbf{r} d\mathbf{p}.$$

in a numerical computation, where the integral in turn is approximated by a sum over many trajectories with initial data sampled from the initial PDF ρ_0. Provided the original Hamiltonian $\mathcal{H}$ and the modified Hamiltonian $\tilde{\mathcal{H}}$ share the same 'qualitative' dynamics, one can expect the two expectation values $\langle A \rangle(t_n)$ and $\langle \tilde{A} \rangle(t_n)$ to be close even over long time intervals. This vague and non-rigorous statement is indeed confirmed by numerous simulation results. For attempts to put such a statement within a rigorous mathematical context see Reich [32] and Tupper [40].

Let us summarize the main points of this section. The Störmer-Verlet method can be written as the concatenation of exact solution maps to a sequence of Hamiltonian functions $\mathcal{H}_i$, $i = 1, 2, 3$. This implies that the Störmer-Verlet method is symplectic and hence is equivalent to the exact solution of a time-dependent modified Hamiltonian problem. For sufficiently small step-sizes this time-dependence averages itself out and an excellent long time conservation of energy is thus observed numerically.

These statements apply to all numerical methods that can be derived by a splitting of a Hamiltonian function $\mathcal{H}$ into exactly solvable parts. One of the most interesting

recent applications of this approach to particle methods is in *rigid body dynamics* and we refer the reader to the publications of Touma & Wisdom [38], Reich [31], and Dullweber, McLachlan & Leimkuhler [8]. Another application is provided by the symplectic multiple-time-stepping methods suggested by Tuckerman, Berne & Martyna [39] and Grubmüller, Heller, Windemuth & Schulten [18] as well as its mollified variants introduced by García-Archilla, Sanz-Serna & Skeel [15] and Izaguirre, Reich & Skeel [23].

For a more complete perspective on symplectic integration methods and classical mechanics, the reader is referred to a text on the subject such as that of Sanz-Serna & Calvo [34], Hairer, Lubich & Wanner [20], and Leimkuhler & Reich [25].

4 Numerical Weather Prediction (NWP)

We now come to numerical weather prediction (NWP) as an emerging application area for particle methods and symplectic time-stepping methods. For an introduction to atmospheric dynamics and its governing equations see Andrews [2]. See also Durran [9] for a discussion of numerical methods.

Specifically, we will discuss an application of the *Hamiltonian particle-mesh* (HPM) *method* of Frank, Gottwald & Reich [10, 11] to a two-dimensional vertical slice model. Such simplified models are commonly used to study non-hydrostatic flow over orography [37, 5].

The HPM method has recently also been applied to the shallow-water equations in spherical geometry [12] and to a two-layer shallow-water model [6].

The only other two publications on particle methods for NWP that we are aware of are Salmon [33] and Gadian [14]. Both references use the SPH method of Lucy [27] and Monaghan & Gingold [17] and apply it to two-dimensional (vertical and horizontal) atmospheric model systems.

4.1 Euler Equations of Atmospheric Motion

The Euler equations for inviscid isentropic motion of a perfect gas in a rotating reference frame can be expressed in the form [9]:

$$\frac{d\mathbf{v}}{dt} = -c_p\theta\nabla_{\mathbf{x}}\pi - g\mathbf{k} - f\mathbf{k}\times\mathbf{v}, \tag{11}$$

$$\frac{d\theta}{dt} = 0, \tag{12}$$

$$\frac{d\pi}{dt} = -\frac{R}{c_v}\pi\nabla_{\mathbf{x}}\cdot\mathbf{v}, \tag{13}$$

where pressure p, as used in the standard formulation of Euler's equations, has been replaced by Exner's function

$$\pi = (p/p_0)^{R/c_p} = \frac{T}{\theta},$$

which gives rise to the relation $\rho^{-1}\nabla_{\mathbf{x}}p = c_p\theta\nabla_{\mathbf{x}}\pi$.

In the preceding, g is the gravitational acceleration, f is twice the angular velocity of the frame of reference [7], $\mathbf{k} = (0,0,1)^T$ is a unit vector pointing in the z-direction for simplicity, $d(\,)/dt = \partial_t(\,) + \mathbf{v}\cdot\nabla_{\mathbf{x}}(\,)$ is the material time derivative, $\mathbf{v} = (u,v,w)^T$ is the three-dimensional velocity vector, $\theta = T\,(p/p_0)^{-R/c_p}$ is the potential temperature, T is the temperature, ρ is the density, $p_0 = 10^5\,\mathrm{pa}$ is a constant reference pressure, R is the gas constant for dry air, c_p is the specific heat at constant pressure, c_v is the specific heat at constant volume, $c_p = R + c_v = 1005\,\mathrm{J\,K^{-1}\,kg^{-1}}$, and $R/c_v \approx 0.4$, $c_p/c_v \approx 1.4$.

Exner's function can also be expressed in the form [9]

$$\pi = \left(\frac{\rho\theta}{\rho_0 T_0}\right)^{R/c_v}.$$

where, T_0 is the surface reference temperature and $\rho_0 = p_0/(T_0 R)$ the reference density at $z = 0$. This suggests to introduce a new density $\mu = \rho\theta/(\rho_0 T_0)$ and to replace the equations (11)-(13) by the modified set

$$\frac{d\mathbf{v}}{dt} = -c_p\theta\nabla_{\mathbf{x}}\pi - g\mathbf{k} - f\mathbf{k}\times\mathbf{v}, \tag{14}$$

$$\frac{d\theta}{dt} = 0, \tag{15}$$

$$\frac{d\mu}{dt} = -\mu\nabla_{\mathbf{x}}\cdot\mathbf{v}, \tag{16}$$

with Exner's function now taking the form $\pi = \mu^{R/c_v}$.

4.2 A Vertical Slice Model

High resolution simulations of atmospheric flows over complex orography pose many difficult numerical problems. Mesoscale and cloud simulations require the use of non-hydrostatic equations and sound waves must be either filtered from the equations or dealt with numerically by the use of implicit or semi-implicit methods [9]. To illustrate the task at hand, it is sufficient to restrict Euler's equation to the (x,z)-plane and to ignore the effect of the Coriolis force [37, 5]. The resulting equations may be written in the form

$$\frac{d\mathbf{u}}{dt} = -c_p\theta\nabla_{\mathbf{x}}\pi - g\mathbf{k}, \tag{17}$$

$$\frac{d\theta}{dt} = 0, \tag{18}$$

$$\frac{d\mu}{dt} = -\mu\nabla_{\mathbf{x}}\cdot\mathbf{u}, \tag{19}$$

where $\mathbf{u} = (u,w)^T$ is the two-dimensional velocity field, $\mathbf{x} = (x,z)^T$ denotes the coordinates in the (x,z)-plane, $\mathbf{k} = (0,1)^T$, and all other quantities are defined as before. These simplified equations are often referred to as a *vertical slice model*.

[7] The angular velocity is assumed, for simplicity, to be constant. This is often referred to as the f-plane approximation. A more realistic approximation is provided by the β-plane approximation $f = f_0 + \beta y$.

Large scale atmospheric flow regimes are characterized by the relative smallness of the vertical acceleration dw/dt compared to the forcing terms on the right hand side of the vertical momentum equation. Given a typical horizontal scale of 1000 km and a vertical scale of 10 km, the vertical acceleration can be estimated by [2]

$$\frac{d}{dt}w \sim 10^{-7}\,\mathrm{m\,s^{-2}},$$

which is much smaller than $g \sim 10\,\mathrm{m\,s^{-2}}$. The only remaining term is $c_p\theta\pi_z$, which then has to be in balance with the gravitational forcing term. Large scale atmospheric simulations may hence make use of the *hydrostatic approximation*

$$c_p\theta\frac{\partial\pi}{\partial z} + g = 0. \tag{20}$$

The hydrostatic approximation is no longer valid for *mesoscale simulations* with a horizontal and vertical length scale resolution between 1 and 10 km, and that is the flow regime we are interested in.

Let us consider a domain of length $L = 80\,\mathrm{km}$ and of height $H = 20\,\mathrm{km}$. The bottom orography is given by an 'Agnesi mountain profile' of the form [5]:

$$h(x) = \frac{h_0}{1 + ((x - x_0)/a)^2} \tag{21}$$

with $h_0 = 1\,\mathrm{km}$, $a = 4\,\mathrm{km}$, and $x_0 = 10\,\mathrm{km}$. For simplicity, we use periodic boundary conditions in the lateral direction. The implementation of top and bottom vertical boundary conditions is more complicated and will be discussed in the context of our numerical method in §4.3 and §4.4.

Even though we wish to solve the non-hydrostatic equations (17)-(19), it is useful to introduce a time-independent *hydrostatic reference state* $(\bar{T}(z), \bar{\theta}(z), \bar{\pi}(z))$ *via* the equations

$$\bar{T} = T_0 - \Gamma z, \quad c_p\bar{\theta}\frac{\partial\bar{\pi}}{\partial z} + g = 0, \quad \bar{T} = \bar{\pi}\,\bar{\theta}, \tag{22}$$

where $\Gamma = 1\,\mathrm{K\,km^{-1}}$ is the lapse rate and $T_0 = 250\,\mathrm{K}$ is the surface reference temperature at $z = 0$. One also defines $\bar{\pi} = 1$ at $z = 0$. See, *e.g.*, [2] for details.

4.3 Hamiltonian Truncation of the Slice Model

The equations (17)-(19) can be discretized by a natural extension of the *Hamiltonian particle-mesh* (HPM) *method* [10, 11]. In particular, given a computational grid $\{\bar{\mathbf{x}}_k = (\bar{x}_k, \bar{z}_k)\}$ and N Lagrangian particles $\{\mathbf{r}_i(t) = (x_i(t), z_i(t))\}$, an approximation to μ at the grid point $\bar{\mathbf{x}}_k$ is provided by

$$\mu_k(t) = \frac{1}{\gamma_k\,\rho_0 T_0}\sum_i m_i\theta_i\,\psi_k(\mathbf{r}_i(t)). \tag{23}$$

Here $\psi_k(\mathbf{x})$ are positive basis functions, which form a partition of unity $\sum_k \psi_k(\mathbf{x}) = 1$, the constants γ_k are defined by $\gamma_k = \int \psi_k(\mathbf{x})d\mathbf{x}$, m_i is the mass of the i-th particle

and θ_i its potential temperature. An important identity is the interpolation formula

$$\pi(\mathbf{x},t) = \sum_k \psi_k(\mathbf{x})\pi_k(t),$$

which implies, for example,

$$\nabla_{\mathbf{x}}\pi(\mathbf{x},t) = \sum_k \pi_k(t)\nabla_{\mathbf{x}}\psi_k(\mathbf{x}).$$

Next we define $e_k = e(\mu_k)$ such that $e'(\mu_k) = c_p\rho_0 T_0 \pi_k$ and $\pi_k = [\mu_k(t)]^{R/c_v}$. A simple calculation yields

$$\nabla_{\mathbf{r}_i}\left(\sum_k \gamma_k e_k(t)\right) = c_p m_i\theta_i \sum_k \pi_k \nabla_{\mathbf{r}_i}\psi_k(\mathbf{r}_i) = c_p m_i\theta_i \nabla_{\mathbf{x}}\pi(\mathbf{x},t)_{|\mathbf{x}=\mathbf{r}_i}.$$

Here the gradient *w.r.t.* $\mathbf{r}_i = (x_i, z_i)^T$ stands for the column vector $\nabla_{\mathbf{r}_i}(\,) = (\partial_{x_i}(\,), \partial_{z_i}(\,))^T$.

Using these identities, the momentum equation (17) is now discretized to

$$\frac{d}{dt}\mathbf{u}_i = -c_p\theta_i \sum_k \pi_k \nabla_{\mathbf{r}_i}\psi_k(\mathbf{r}_i) - g\mathbf{k}, \tag{24}$$

and particles are advected according to

$$\frac{d}{dt}\mathbf{r}_i = \mathbf{u}_i, \tag{25}$$

for $i = 1, \ldots, N$. Upon introducing canonical momenta $\mathbf{p}_i = m_i\mathbf{u}_i$, the discrete equations of motion become Hamiltonian with conserved energy

$$\mathcal{H} = \frac{1}{2}\sum_i m_i^{-1}\|\mathbf{p}_i\|^2 + g\sum_i m_i\mathbf{k}\cdot\mathbf{r}_i + \sum_k \gamma_k e(\mu_k).$$

A key aspect of the HPM method is the introduction of an appropriate *smoothing operator* that filters out numerically induced small scale (sub-grid) disturbances [10, 11]. Smoothing, as used in the original HPM method, can be achieved by introducing the smoothed/filtered density $\tilde{\mu} = \left(1 - \alpha^2\nabla^2\right)^{-1}\mu$ and its corresponding numerical approximation

$$\tilde{\mu}_k = a_{kl}\mu_l, \tag{26}$$

where $\{a_{kl}\}$ is a discrete approximation to the inverse modified Helmholtz operator.

The subsequent discussion assumes that simulations start from a hydrostatic reference state defined by (22). The above smoothing procedure is not optimal under such circumstances and the following refined implementation is suggested instead. Given $\bar{\pi}_k = \bar{\pi}(z_k)$, we define the (constant) potential temperature θ_i of particle $\mathbf{r}_i$ at the initial time *via* the *computational reference state*:

$$g + c_p\theta_i \sum_k \bar{\pi}_k \frac{\partial}{\partial z_i}\psi_k(\mathbf{r}_i) = 0.$$

The mass m_i of particle $\mathbf{r}_i$ is defined according to the initial density of the fluid. We then compute $\mu_k(0)$ as in (23) and set $\bar{\mu}_k = \mu_k(0)$. The quantities $\bar{\pi}_k$ and $\bar{\mu}_k$ are kept constant throughout the simulation.

Now the discrete momentum equation (24) is replaced by

$$\frac{d}{dt}\mathbf{u}_i = -c_p\theta_i \sum_k \left\{ \bar{\pi}_k + \sum_l a_{kl}\left[\pi(\tilde{\mu}_l) - \pi(\bar{\mu}_l)\right] \right\} \nabla_{\mathbf{r}_i}\psi_k(\mathbf{r}_i) - g\mathbf{k},$$

where

$$\pi(\tilde{\mu}_k) = (\tilde{\mu}_k)^{R/c_v}, \qquad \pi(\bar{\mu}_k) = (\bar{\mu}_k)^{R/c_v},$$

with

$$\tilde{\mu}_k = \bar{\mu}_k + \sum_l a_{kl}(\mu_l - \bar{\mu}_l).$$

We assume that $\bar{\pi}_k \approx \pi(\bar{\mu}_k)$.

The reason for this somewhat complicated looking smoothing procedure is twofold: (i) The equations of motion can be derived from a Hamiltonian function

$$\begin{aligned}\mathcal{H} \;=\; & \frac{1}{2}\sum_i m_i^{-1}\|\mathbf{p}_i\|^2 + g\sum_i m_i\mathbf{k}\cdot\mathbf{r}_i + \\ & \sum_k \left[\gamma_k e(\tilde{\mu}_k) + c_p \sum_i \theta_i m_i \psi_k(\mathbf{r}_i) \left\{ \bar{\pi}_k - \sum_l a_{kl}\pi(\bar{\mu}_l) \right\} \right].\end{aligned}$$

(ii) Smoothing is applied only to deviations from the reference state.

The physical domain is restricted to 80 km in the horizontal and 20 km in the vertical. Periodic boundary conditions are applied at the lateral boundaries. To mimic the atmosphere above 20 km height, we introduce a 2 km layer of ghost particles with mass m_k and potential temperature θ_k according to the hydrostatic reference state. These ghost particles do not move but contribute to the Exner function π_k and the density μ_k near the top boundary. A 2 km layer of ghost particles is also added to the bottom of the physical domain. Hence the computational domain is $(0, 80] \times [-2, 22]$ (in km).

The bottom orography is modeled by a strongly repulsive potential and a friction force that acts normal to the boundary, *i.e.*

$$V^B(\mathbf{r}_i) = \beta m_i \sum_k \psi_k(\mathbf{r}_i)\, \mathrm{e}^{-\alpha(\bar{z}_k - h(\bar{x}_k))} \tag{27}$$

and

$$\mathbf{F}_i^R = -\gamma m_i \nabla_{\mathbf{r}_i} g(\mathbf{r}_i)\, (\nabla_{\mathbf{r}_i} g(\mathbf{r}_i)\cdot\mathbf{u}_i), \qquad g(\mathbf{r}_i) = \sum_k \psi_k(\mathbf{r}_i)\, \mathrm{e}^{-\delta(\bar{z}_k - h(\bar{x}_k))},$$

with positive constants $\beta = 0.025\,\mathrm{J\ kg^{-1}}$, $\gamma = 0.9\,\mathrm{s^{-1}}$, $\alpha = 80\,\mathrm{km^{-1}}$, $\delta = 2\,\mathrm{km^{-1}}$. The function h is as defined in (21).

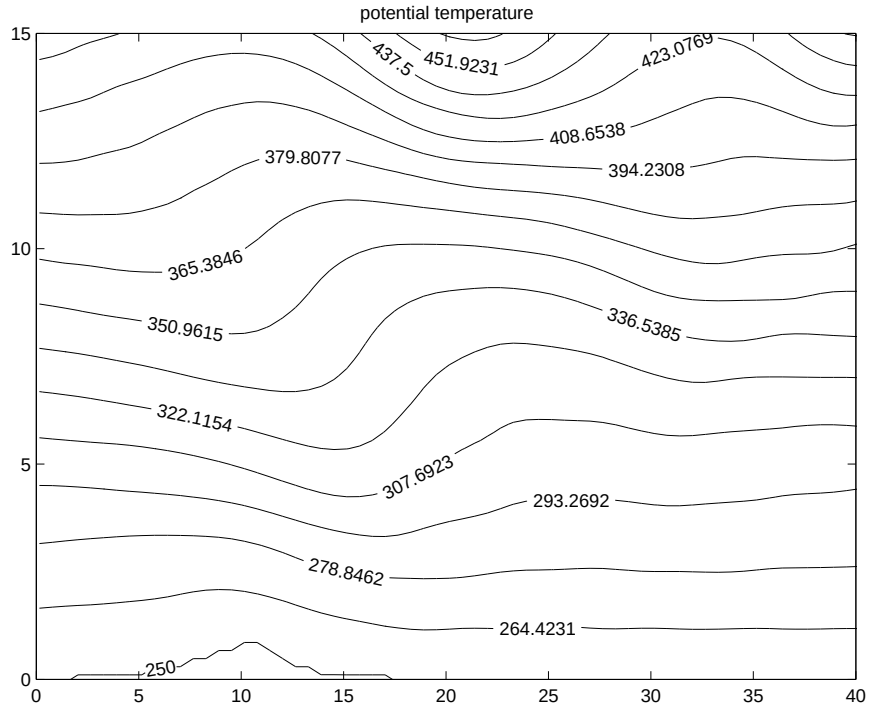

Fig. 1 Contour lines of constant potential temperature θ [K] after one hour displayed over a domain $(x, z) \in [0, 40\,\mathrm{km}] \times [0, 15\,\mathrm{km}]$.

4.4 Numerical Experiment

We performed a numerical experiment for $h_0 = 1\,\mathrm{km}$ and $a = 4\,\mathrm{km}$ in (21), $w_i(0) = 0$, $u_i(0) = 0$, and all particles initially in hydrostatic balance. The horizontal velocities u_i of all particles were incremented by a constant value over a period of 15 min such that the total increment was $u = 72\,\mathrm{km/h}$. The computational domain was discretized by a 256×256 grid and 9 particles per cell at time $t = 0$. The grid corresponds to a horizontal mesh-size of $\Delta x \approx 300\,\mathrm{m}$ and a vertical mesh-size of $\Delta z \approx 100\,\mathrm{m}$.

All particles with $\|\nabla_{\mathbf{r}_i} V^B(\mathbf{r}_i(0))\|/m_i > 10^{-5}\,\mathrm{m/s^2}$, $z_i(0) > 20\,\mathrm{km}$ or $z_i(0) < 0$ were treated as passive ghost particles. A modified inverse Helmholtz operator was used as the smoothing operator with a smoothing length $\alpha_x = 750\,\mathrm{m}$ in the x-direction and $\alpha_z = 500\,\mathrm{m}$ in the z-direction. The operator was implemented using a 2D FFT over the computational domain. The equations of motion were integrated by the Störmer-Verlet method over a total of one hour using a time-step of $\Delta t = 2\,\mathrm{s}$. The potential temperature distribution at the final simulation time is shown in Fig. 1. The final values of the horizontal velocity field are displayed in Fig. 2.

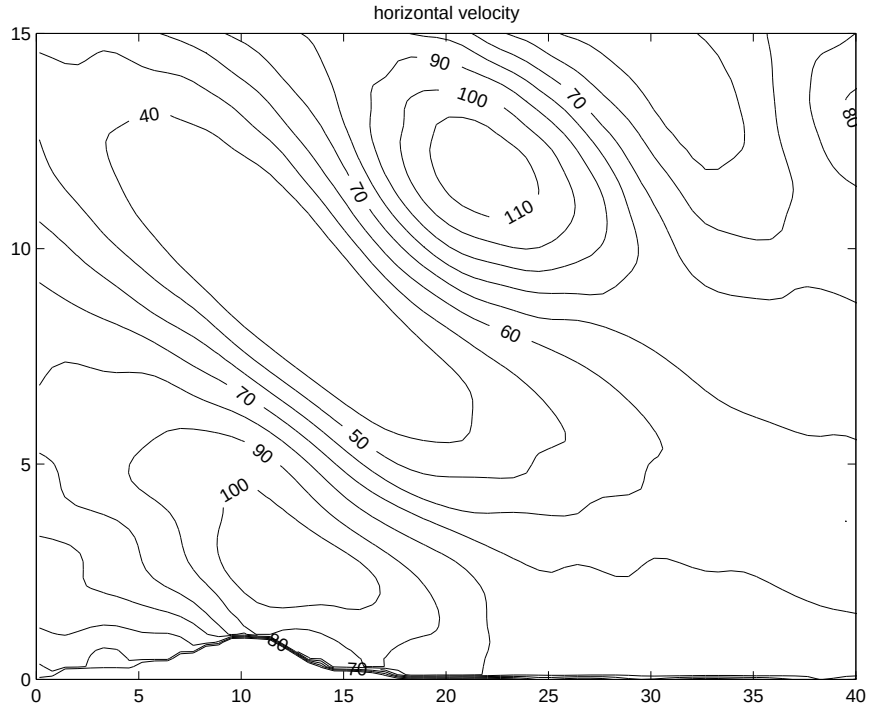

Fig. 2 Contour lines of constant horizontal velocity u [km/h] after one hour displayed over a domain $(x, z) \in [0, 40\,\mathrm{km}] \times [0, 15\,\mathrm{km}]$.

Appendix (Hamiltonian Mechanics)

Let $\mathbf{r}$ denote an n-vector of particle positions and $\mathbf{p}$ the associated vector of conjugate momenta. Given a Hamiltonian $\mathcal{H}$ the associated canonical Hamiltonian equations of motion are

$$\dot{\mathbf{r}} = +\nabla_{\mathbf{p}}\mathcal{H}(\mathbf{r}, \mathbf{p}), \qquad \dot{\mathbf{p}} = -\nabla_{\mathbf{r}}\mathcal{H}(\mathbf{r}, \mathbf{p}).$$

Upon concatenating the positions $\mathbf{r}$ and the momenta $\mathbf{p}$ into one vector $\mathbf{z} = (\mathbf{r}^T, \mathbf{p}^T)^T \in \mathbb{R}^{2n}$, the Hamiltonian equations can be condensed into the compact form

$$\dot{\mathbf{z}} = \mathbf{J}\nabla_{\mathbf{z}}\mathcal{H}(\mathbf{z}), \quad \mathbf{J} = \begin{bmatrix} \mathbf{0}_n & \mathbf{I}_n \\ -\mathbf{I}_n & \mathbf{0}_n \end{bmatrix}.$$

The linearized equations along $\mathbf{z}(t)$ are given by

$$\dot{\mathbf{Z}} = \mathbf{J}\mathbf{A}(t)\,\mathbf{Z}, \qquad \mathbf{A}(t) = D_{\mathbf{zz}}H(\mathbf{z}(t)).$$

Let $\mathbf{V}(t) \in \mathbb{R}^{2n}$ and $\mathbf{U}(t) \in \mathbb{R}^{2n}$ denote any two solutions of the linearized equations. Note that the matrix $\mathbf{J}$ is skew-symmetric while $\mathbf{A}(t)$ is symmetric. Then one can

easily verify that

$$\frac{d}{dt}\left[\mathbf{V}(t)^T\mathbf{J}^{-1}\mathbf{U}(t)\right] = 0.$$

The *symplectic two-form* Ω is now defined by

$$\Omega(\mathbf{U},\mathbf{V}) = \mathbf{U}^T\mathbf{J}^{-1}\mathbf{V}.$$

Hence conservation of symplecticness (*i.e.* $\dot{\Omega} = 0$) can be concluded along solutions of the linearized equations.

A similar procedure applies to maps. Given a map Φ the linearization (Jacobian matrix) can be used to propagate two vectors $\mathbf{U}^n$ and $\mathbf{V}^n$. The map Φ is called *symplectic* if

$$\Omega(\mathbf{U}^{n+1},\mathbf{V}^{n+1}) = \Omega(\mathbf{U}^n,\mathbf{V}^n).$$

For planar maps conservation of sympleticness is equivalent to conservation of area. For higher dimensional maps this analogy becomes slightly more complex but a consequence is conservation of volume in phase space.

The idea that a numerical method for classical mechanics should preserve the symplectic two-form can first be found in a technical report by VOGELAERE [7].

References

[1] M.P. Allen and D.J. Tildesley. *Computer Simulation of Liquids*. Clarendon Press, Oxford, 1987.

[2] D.G. Andrews. *An Introduction to Atmospheric Physics*. Cambridge University Press, Cambridge, 2000.

[3] V.I. Arnold. *Mathematical Methods of Classical Mechanics*. Springer-Verlag, New York, 2nd edition, 1989.

[4] G. Benetin and A. Giorgilli. On the Hamiltonian interpolation of near to the identity symplectic mappings with application to symplectic integration algorithms. *J. Stat. Phys.*, 74:1117–1143, 1994.

[5] L. Bonaventure. A semi-implicit semi-Lagrangian scheme using the height coordinate for a nonhyrostatic and fully elastic model of the atmosphere. *J. Comput. Phys.*, 158:186–213, 2000.

[6] C.J. Cotter, J. Frank, and S. Reich. Hamiltonian particle-mesh method for two-layer shallow-water equations subject to the rigid-lid approximation. *SIAM J. Appl. Dyn. Sys*, 3, 2004.

[7] R. de Vogelaere. Methods of integration which preserve the contact transformation property of the Hamiltonian equations. Technical Report 4, Dept. Math. Univ. of Notre Dame, 1956.

[8] A. Dullweber, B. Leimkuhler, and R.I. McLachlan. Split-Hamiltonian methods for rigid body molecular dynamics. *J. Chem. Phys.*, 107:5840–5851, 1997.

[9] D.R. Durran. *Numerical Methods for Wave Equations in Geophysical Fluid Dynamics*. Springer-Verlag, Berlin Heidelberg, 1998.

[10] J. Frank, G. Gottwald, and S. Reich. The Hamiltonian particle-mesh method. In M. Griebel and M.A. Schweitzer, editors, *Meshfree Methods for Partial Differential Equations, Lecture Notes in Computational Science and Engineering*, volume 26, pages 131–142, Berlin Heidelberg, 2002. Springer-Verlag.

[11] J. Frank and S. Reich. Conservation properties of smoothed particle hydrodynamics applied to the shallow-water equations. *BIT*, 43:40–54, 2003.
[12] J. Frank and S. Reich. The Hamiltonian particle-mesh method for the spherical shallow water equations. *Atmospheric Science Letters*, 5:89–95, 2004.
[13] D. Frenkel and B. Smit. *Understanding Molecular Simulation*. Academic Press, New York, 2nd edition, 2001.
[14] A.M. Gadian, J. Dormand, and J.S.A. Green. Smoothed-particle hydrodynamics as applied to 2D plume convection. *Atmospheric Research*, 24:289–304, 1989.
[15] B. García-Archilla, J.M. Sanz-Serna, and R.D. Skeel. The mollified impulse method for oscillatory differential equations. *SIAM J. Sci. Comput.*, 20:930–963, 1998.
[16] R.A. Gingold and J.J. Monaghan. Smoothed Particle Hydrodynamics: Theory and application to non-spherical stars. *Mon. Not. R. Astr. Soc.*, 181:375–389, 1977.
[17] R.A. Gingold and J.J. Monaghan. Smoothed particle hydrodynamics: theory and application to non-spherical stars. *Mon. Not. R. Astr. Soc.*, 181:375–389, 1977.
[18] H. Grubmüller, H. Heller, A. Windemuth, and K. Schulten. Generalized Verlet algorithm for efficient molecular dynamics simulations with long-range interactions. *Mol. Sim.*, 6:121–142, 1991.
[19] E. Hairer and Ch. Lubich. The life-span of backward error analysis for numerical integrators. *Numer. Math.*, 76:441–462, 1997.
[20] E. Hairer, Ch. Lubich, and G. Wanner. *Geometric Numerical Integration*. Springer-Verlag, Berlin Heidelberg, 2002.
[21] E. Hairer, Ch. Lubich, and G. Wanner. Geometric numrical integration by the Störmer-Verlet method. *Acta Numerica*, 12:399–450, 2003.
[22] R.W. Hockney and J.W. Eastwood. *Computer Simulations Using Particles*. Institute of Physics Publisher, Bristol and Philadelphia, 1988.
[23] J.A. Izaguirre, S. Reich, and R.D. Skeel. Longer time steps for molecular dynamics. *J. Chem. Phys.*, 110:9853–9864, 1999.
[24] S. Kuksin and J. Pöschel. On the inclusion of analytic symplectic maps in analytic Hamiltonian flows and its applications. In S. Kuksin, V. Lazutkin, and J. Pöschel, editors, *Seminar on Dynamical Systems (St. Petersburg, 1991)*, volume 12 of *Progr. Nonlinear Differential Equations Appl.*, pages 96–116, Basel, 1994. Birkhäuser Verlag.
[25] B. Leimkuhler and S. Reich. *Geometric Numerical Methods for Hamiltonian Mechanics*. Cambridge University Press, Cambridge, 2004.
[26] L.B. Lucy. A numerical approach to the testing of the fission hypothesis. *Astron. J.*, 82:1013–1024, 1977.
[27] L.B. Lucy. A numerical approach to the testing of the fission hypothesis. *Astron. J.*, 82:1013–1024, 1977.
[28] P.C. Moan. On the KAM and Nekhoroshev theorems for symplectic integrators and implications for error growth. *Nonlinearity*, 17:67–83, 2004.
[29] B.E. Moore and S. Reich. Backward error analysis for multi-symplectic integration methods. *Numer. Math.*, 95:625–652, 2003.
[30] A.I. Neishtadt. The separation of motions in systems with rapidly rotating phase. *J. Appl. Math. Mech.*, 48:133–139, 1984.
[31] S. Reich. Symplectic methods for conservative multibody systems. In J.E. Mardsen, G.W. Patrick, and W.F. Shadwick, editors, *Integration Algorithms and Classical Mechanics*, volume 10 of *Fields Inst. Com.*, pages 181–192. Amer. Math. Soc., 1996.
[32] S. Reich. Backward error analysis for numerical integrators. *SIAM J. Numer. Anal.*, 36:475–491, 1999.
[33] R. Salmon. Practical use of Hamilton's principle. *J. Fluid Mech.*, 132:431–444, 1983.
[34] J.M. Sanz-Serna and M.P. Calvo. *Numerical Hamiltonian Problems*. Chapman & Hall, London, 1994.

[35] T. Schlick. *Molecular Modeling and Simulation*. Springer-Verlag, New-York, 2002.
[36] R.D. Skeel and D.J. Hardy. Practical construction of modified Hamiltonians. *SIAM J. Sci. Comput.*, 23:1172–1188, 2001.
[37] J.M. Straka, R.B. Wihhelmson, L.J. Wicker, J.R. Anderson, and K.K. Doegemeier. Numerical solutions of a non-linear density current: A benchmark solution and comparison. *Int. J. Numer. Methods Fluids*, 17:1–22, 1993.
[38] J. Touma and J. Wisdom. Lie-Poisson integrators for rigid body dynamics in the solar system. *Astron. J.*, 107:1189–1202, 1994.
[39] M. Tuckerman, B.J. Berne, and G.J. Martyna. Reversible multiple time scale molecular dynamics. *J. Chem. Phys.*, 97(3):1990–2001, 1992.
[40] P. Tupper. Ergodicity and numerical simulation. Technical report, McGill University, 2004.